MATERIAL STRENGTH EFFECTS ON SHAPED CHARGE TIP VELOCITIES

N. Ouye, D. Boeka, and S. Hancock

General Dynamics-OTS, 2950 Merced Street, Suite 131
San Leandro, CA 94577-0205

A test and computational study has been made which compares the sensitivity to strength of the tip velocity of a Molybdenum hemisphere and cone. The two primary factors that have been identified for the higher strength sensitivity of the hemisphere compared to the cone are (1) a greater sensitivity to loss of energy to plastic work during liner collapse due to its late time of tip formation and (2) a larger resistance to the stretching of the jet due to a high ratio of flow stress to peak stagnation pressure.

INTRODUCTION

In many shaped charge (SC) devices, the tip velocity is relatively insensitive to the liner strength. High-performance SCs that use Molybdenum (Mo) liners documented in References [1], [2], and [3] indicate this insensitivity to manufacturing methods, grain size, and strength. However, recently a Molybdenum (Mo) hemispherical shaped charge showed a very high sensitivity of tip velocity to strength. A study was made to identify the primary factors which caused this high strength sensitivity because of the importance of tip velocity on shaped charge performance.

To provide a set of data which could be compared with computer modeling, tests were done with Mo hemispherical liners with several different fabrication histories, with a hemisphere having identical geometry but made of copper (Cu), and with a Mo cone of the same diameter. The computer modeling used the CALE [4] hydrocode which has been successfully used for many previous shaped charge designs like General Dynamics OTS' K-Charge [5]. For a variety of liner shapes, including tulips, trumpets, and cones, past test results have validated the analytical jet tip velocity predictions with errors of less than 0.3 km/s for Cu and Mo liner materials.

TEST DATA

Figure 1 shows two shaped charge designs that will be discussed and compared, a hemisphere and a 60° cone, each with a charge diameter of ~18mm. Figure 2 shows the jet x-ray for the Mo conical liner with its indicated tip and tail velocities.
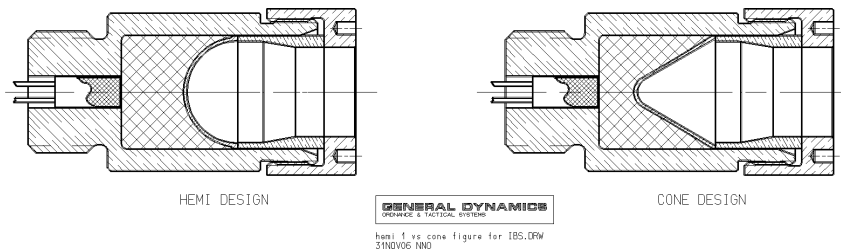

HEMI DESIGN   GENERAL DYNAMICS   CONE DESIGN
                            ORDNANCE & TACTICAL SYSTEMS
                            hemi 1 vs cone figure for IBS.DRW
                            31NOV06 NNO

FIGURE 1 Hemi and Cone Designs

Vtail = 2.8 km/s   Vtip = 6.8 km/s
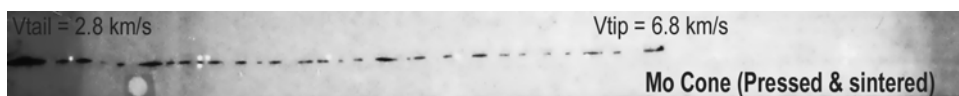
Mo Cone (Pressed & sintered)

FIGURE 2 Jet X-ray for Mo Conic Liner

Figure 3 shows x-rays of jets produced from hemispheres of Mo which were fabricated from material with three different processing histories. The tip velocities vary from 4.1 km/s for a liner machined from a pressed and sintered preform and also from unannealed barstock, to 4.8 km/s for annealed bar stock. This indicates that the jet tip velocity in this hemispherical design is sensitive to the material strength.
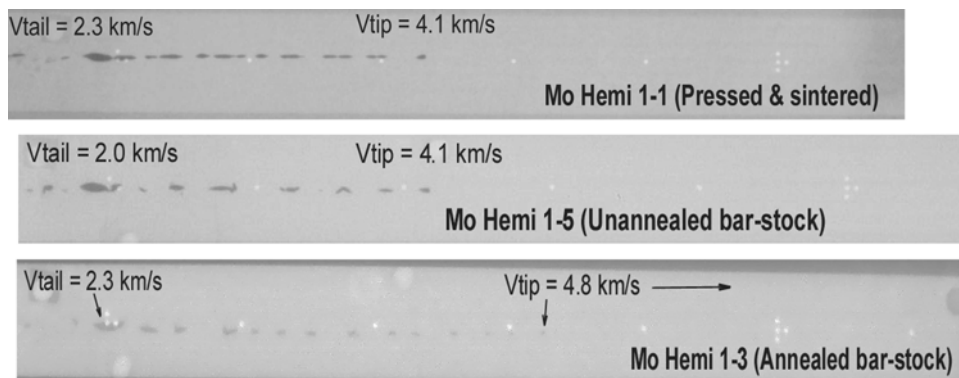

Vtail = 2.3 km/s   Vtip = 4.1 km/s

Mo Hemi 1-1 (Pressed & sintered)

Vtail = 2.0 km/s   Vtip = 4.1 km/s

Mo Hemi 1-5 (Unannealed bar-stock)

Vtail = 2.3 km/s   Vtip = 4.8 km/s

Mo Hemi 1-3 (Annealed bar-stock)

FIGURE 3 Jet X-rays for Mo Hemi Liners with Different Starting Material States

An additional data point is provided by a hemispherical liner of exactly the same geometry but manufactured from Cu. In this case the tip velocity was 5.5 km/s, which is

much higher than for the Mo hemispheres and a further indication of strength sensitivity.

COMPUTATIONAL STUDIES

Figure 4 shows jets computed for the hemisphere and cone using three material property assumptions: strengthless Mo, Cu, and Mo. Although the strengthless Mo calculations are not physically realistic, they provide a useful reference. The Cu liner is computed using the Steinberg-Guinan model [6] and the Mo liner uses the Steinberg-Lund rate-dependent model [7], both with the CALE library properties. The jets are displayed in order of increasing strength. While both liner geometries shows a decrease in the tip velocity as strength increases, the effect is much more pronounced for the hemispherical liner, clearly indicating that the loss in tip velocity is due to an overall loss in jet kinetic energy rather than being a localized effect at the tip.
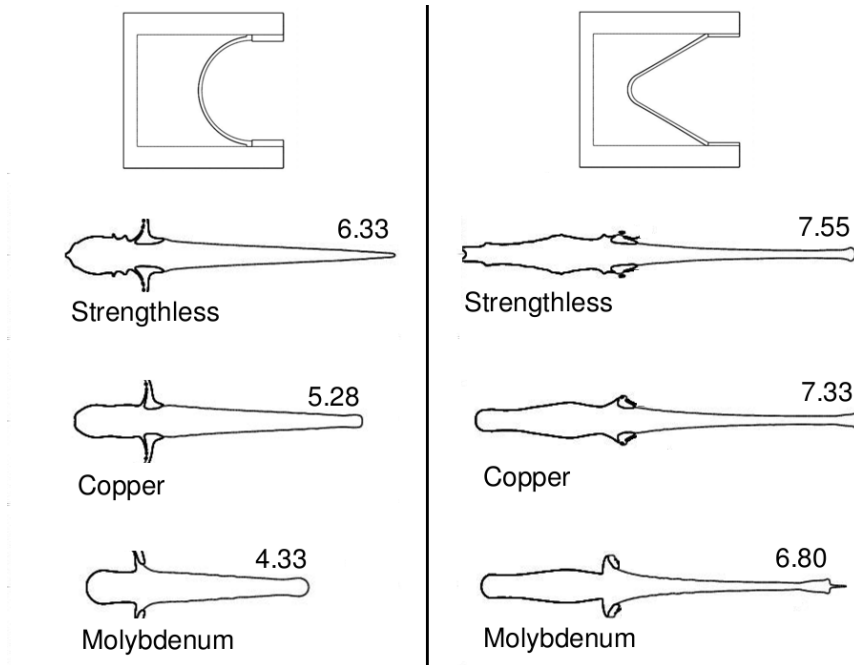
The hemispherical jets are shown at t=10 μs and the conical jets are shown at t=9 μs.

FIGURE 4. Jets computed with different strength assumptions.

Table 1 compares the computed tip velocities with the test data.

TABLE 1 Comparison of Tip Velocitiy Data and Computations

Material	Liner Geometry	Measured Tip, Km/s	Calculated Tip, Nominal Properties, km/s
Mo pressed and sintered	Cone	6.8	6.8
Mo pressed and sintered	Hemisphere	4.1	4.3
Mo unannealed bar stock	Hemisphere	4.1	4.3
Mo annealed bar stock	Hemisphere	4.8	4.3
Copper	Hemisphere	5.5	5.3

These comparisons show that the calculations are fairly accurate except for the Mo annealed bar stock. The spread in the hemisphere tip velocities is consistent with a spread in strength properties, and the desire is to understand the primary factors that cause this high sensitivity to strength.

Several analytical studies were done to eliminate possible causes. A mesh refinement study showed that the predicted tip is insensitive to the assumed mesh size. Table 2 shows that other assumptions for the Mo model do not significantly change the predicted tip velocity for the hemisphere. Calculations were made with the Steinberg-Lund rate-dependent model of devices scaled up by a factor of 10, to a 180 mm charge diameter. The Mo hemisphere tip increased slightly from 4.33 km/s to 4.40 km/s, and the cone's tip velocity remained unchanged, indicating that the high jet tip sensitivity of the Mo hemisphere is not a size or rate effect.

TABLE 2 Tip Velocity of Mo Hemisphere computed with Several Models

Model	Tip Velocity, km/s
Steinberg-Lund, rate dependent	4.33
Steinberg-Guinan, rate independent	4.40
Constant 1.6 Gpa	4.30

Figure 5 shows the computed time history of tracer particles entering the tip for the Mo hemisphere and cone, both with and without strength. The tracer locations shown are representative of the tip conditions. The initial tracer location for the cone is slightly above the centerline to insure that it becomes part of the solid tip. Both sets of curves show an inital sharp rise due to the arrival of the detonation wave, followed by a second rapid rise as the particle is accelerated by the stagnation region and enters the jet. When strength is involved, the tip velocity reaches a peak and then decreases as the jet stretches, with a much greater decay in velocity for the hemisphere. For the strengthless hemisphere there is no decrease in velocity after the particle enters the tip, but for the cone there is a slight decrease due to a momentum redistribution from an inverse gradient in the initial jet velocity.
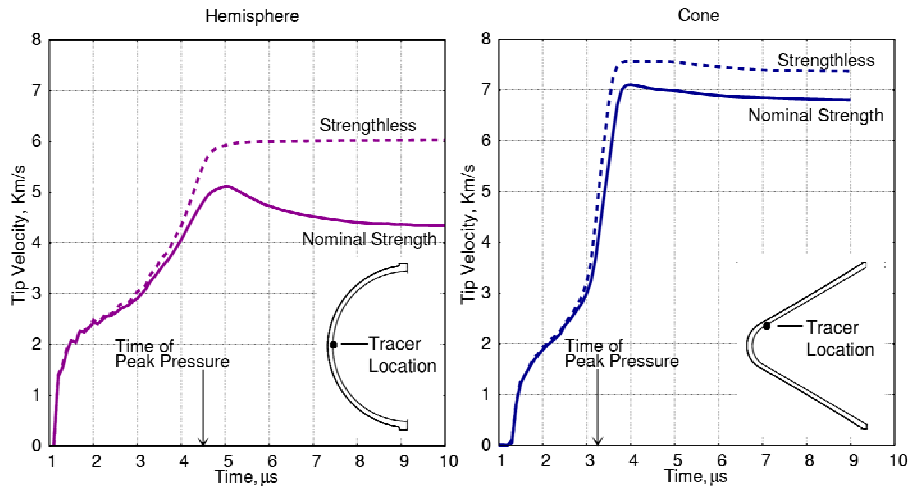
FIGURE 5 Time History of Tip Velocity for Mo Hemi Liner

The difference between the late time tip velocity for the models with and without strength gives a measure of the sensitivity of the two devices to strength. This difference is about three times greater for the hemisphere than for the cone. The origins of this difference were evaluated by examining first the difference between the terminal strengthless tip velocity and the early-time peak tip velocity with strength (liner collapse loss), and second the decay in tip velocity from its early peak to its late-time value (jet stretching loss).

Liner Collapse Loss

The hemispherical liner collapses into a fairly compact mass that causes a peak stagnation pressure to be reached at about 4.5 μs. The jet tip reaches a peak velocity shortly after this time, and fastest portion of the jet remains at the front during the entire tip formation. On the other hand, the jet of the cone forms by the more classical quasi-steady jetting mechanism in which the liner collapses sequentially onto the centerline from apex to base. The tip forms from the apex region, much earlier time than the hemisphere. Peak stagnation pressure occurs at 3.25 μs for the cone and peak tip velocity is reached shortly afterwards. Slower tip material formed earlier is pushed away into a cloud of debris by the faster trailing material.

The modeling results suggest that the greater strength sensitivity of the hemisphere is related to the relatively late formation of its tip. For example, the entire hemisphere inside surface reaches its peak inward velocity before the stagnation pressure peaks. This allows more plastic work before tip formation and hence there is less liner collapse kinetic energy available to drive the jet. On the other hand, only a

portion of the conic liner had reached its peak inward velocity before stagnation pressure peaked. The tip of the cone forms early and it draws its energy more locally from the apex region which has less loss of energy to plastic work due to its smaller initial radius.

The loss of liner kinetic energy due to strength during liner collapse causes a corresponding loss in stagnation pressure. Table 3 shows how stagnation pressure depends upon strength for the hemisphere and the cone. While the absolute drop in peak stagnation pressure is about 8 GPa for both devices over this range of strength, the relative pressure loss is much greater for the hemisphere and this causes a greater loss in its tip velocity.

TABLE 3 Peak Stagnation Pressure, GPa

	Hemisphere	Cone
Strengthless	30	65
Nominal Mo	22	57

Jet Stretching Loss

The conical jet tip moves away from the stagnation region much faster than the hemispherical tip. The axial stress must fall to zero at the jet tip, so the faster the tip departs from the stagnation region, the faster the axial stress gradient decays, and the lower the resistance to stretching. While there are other important factors such as the initial jet diameter, the jet lengthening rate does seem to play a key role.

In classical jet formation theory the rate of this jet lengthening is the velocity (U) of material flowing into and out of the stagnation region. The tip velocity loss during stretching should equivalently be correlated to the peak stagnation pressure (P), which is theoretically proportional to the square of the flow velocity, Thus, for a given material, a device with low stagnation pressure should be more sensitive to strength during the stretching phase. Table 3 indicates that the Mo hemisphere has a much lower stagnation pressure than the cone, verifying this correlation.

Correlation of Tip Loss with Flow Stress-to-Peak Stagnation Pressure Ratio (Y/P)

During the liner collapse phase, the peak stagnation pressure decreases in response to any loss in inward flow velocity, and during the jet stretching phase, the peak stagnation pressure controls the rate of lengthening of the jet and hence the rate of decay of the axial stress gradient. This suggests that the ratio of the flow stress to peak stagnation pressure, *Y/P*, should be a meaningful measure of the effect of strength during both phases of the dynamics.

Calculations were made with Mo and Cu hemispheres and Mo cones for a range of strengths, and the resulting tip velocity losses, both initial and total, were tabulated along with the peak stagnation pressures. A constant flow stress model and nominal Steinberg-Guinan model were used to define the flow stress. The two methods gave very similar results because the tip velocities for these devices are not very sensitive to thermal softening. Figure 6 shows the results for the Mo hemisphere with the tip velocity loss normalized to the velocity V_0 =6.33 km/s (computed for the strengthless material) and plotted against $(Y/P)^{1/2}$. The tip velocity loss of this device during the collapse phase is about 50% greater than the loss during the jet stretching phase. The two contributing loss factors were about equal for the Mo cone.

A comparison of the total loss for each of the cases is shown in Figure 7. The tip velocity losses are normalized to the computed strengthless tip velocities V_0 for the individual designs. The curves for the Cu and Mo hemispheres are very close, which suggests that these curves are almost entirely defined by the liner geometry and the normalized flow stress rather than any other material properties. This figure summarizes the primary reasons that this particular Mo hemisphere is so much more sensitive to strength than the cone. First, the loss curve for the hemisphere shows about twice strength sensitivity as the curve for the cone. Second, the particular hemisphere under study has a much lower stagnation pressure than the cone, so its Y/P ratio is much higher, indicating that strength plays a much larger role in resisting the stretching of the jet for the hemisphere. The combination of these two factors causes the total loss for the Mo hemisphere to be about three times greater than for the Mo cone.

Other shaped charge devices will have different curves because the liner collapse and jet stretching processes are complex and varied. However, when we examined the strength sensitivity of several other devices with higher stagnation pressures, including hemispheres, we found that they follow curves fairly similar to these.
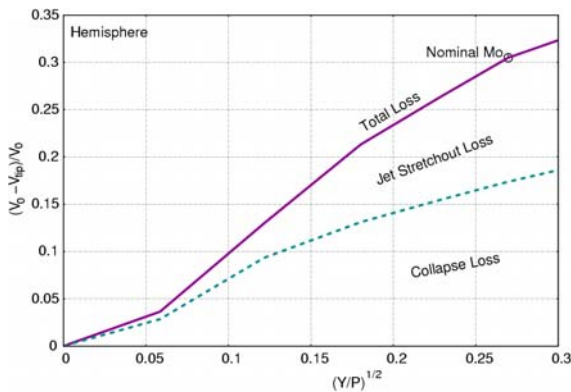

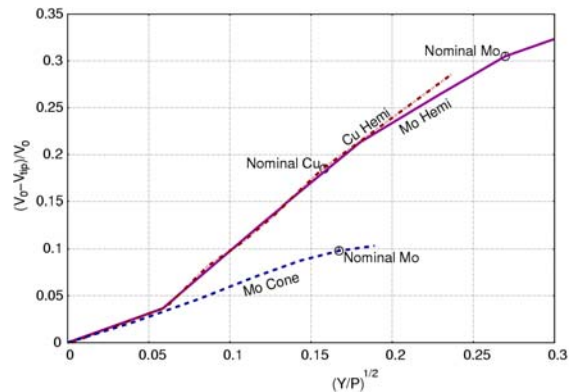**FIGURE 6 Composition of Tip Velocity Loss for Hemisphere**

FIGURE 7 Effect of Strength on Total Tip Velocity Loss

CONCLUSION

The jet tip sensitivity to material strength of two particular devices, a hemisphere and a cone, was examined. The late tip formation time and low stagnation pressure of the hemisphere have been identified as the two primary factors for its high strength sensitivity. It was found that strain rate effects and thermal softening were of secondary importance for the strength sensitivity of these devices. The ratio of the average flow stress during liner collapse to peak stagnation pressure was found to be a useful dimensionless measure of the effect of strength on tip velocity.

While these results are for specific devices and materials, the qualitative results should be more generally applicable and may be useful for understanding the circumstances under which strength may play a large role in determining the tip velocity.

REFERENCES

[1]   Baker, E. L.; Voorhis, G.P.; Campbell, R.; Choi, C.S.; "Development of Molybdenum Shaped Charge Liners Producing High Ductility Jets"; *14th International Ballistic Symposium*; Quebec, Canada; September 1993.

[2]   Cowan, K. G., Bourne, B.; "Analytical Code and Hydrocode Modelling and Experimental Characterization of Shaped Charges Containing Conical Molybdenum Liners"; *19th International Ballistic Symposium*; Interlaken, Switzerland; May 1993.

[3]   Daniels, A. S.; Baker; E. L., Ng, K.W.; Vuong, T.H.; DeFisher, S.E.; "High Performance Trumpet Lined Shaped Charge Technology"; *21th International Ballistic Symposium*; Adelaide, Australia; April 2004

[4]   Tipton, R.; "CALE User's Manual", Lawrence Livermore National Laboratory, 1997

[5]   Mattsson, K.; Sorensen, J.; Ouye, N.; Funston, R. (1999); "Development of the K-Charge, a Short L/D Shaped Charge," *18th International Ballistic Symposium*; San Antonio, TX; November 1999.

[6]   Steinberg D.J.; Cochran, S.G.; and Guinan, M. W.; "Constitutive Model for Metals Applicable at High-Strain Rate", *Journal of Applied Physics.,* **51**, 1498 (1980)

[7]   Steinberg, D.J.; and Lund, C. M.; *Journal of Applied Physics.,* **65**, 1528 (1989)